

Lecture notes on topological insulators

Ming-Che Chang

Department of Physics,
National Taiwan Normal University, Taipei,
Taiwan

(Dated: December 20, 2023)

CONTENTS

I. Electromagnetic response of Weyl semimetal	1
A. Landau levels in magnetic field	1
B. Weyl orbit	2
C. Chiral anomaly	2
D. Chiral magnetic effect	3
E. Negative magnetoresistance	4
F. Semiclassical analysis	4
1. Equation of motion	4
2. Density of states in phase space	4
3. Chiral magnetic effect	5
4. Chiral anomaly	6
References	6

I. ELECTROMAGNETIC RESPONSE OF WEYL SEMIMETAL

The Weyl nodes in a solid lead to several interesting effects. One is the anomalous Hall effect mentioned in previous chapter. The others are, for example, chiral anomaly, and chiral magnetic effect. Before introducing these two effects, let's first study the Landau levels in a Weyl semimetal.

A. Landau levels in magnetic field

Consider a Weyl node with helicity χ ,

$$\mathbf{H} = \chi v \boldsymbol{\sigma} \cdot \mathbf{p}. \quad (1.1)$$

In the presence of a magnetic field $\mathbf{B} = B\hat{z}$, the Hamiltonian becomes (Zyuzin and Burkov, 2012),

$$\mathbf{H} = \chi v (\sigma_x \pi_x + \sigma_y \pi_y) + \chi v \sigma_z p_z, \quad (1.2)$$

where $\boldsymbol{\pi} = \frac{\hbar}{i} \nabla + e\mathbf{A}$, and

$$[\pi_x, \pi_y] = \frac{\hbar e B}{i}. \quad (1.3)$$

The state along z -direction can be just a plane wave $e^{ik_z z}$.

Introduce the creation and annihilation operators,

$$\begin{cases} a = \frac{1}{\sqrt{2\hbar e B}} (\pi_x - i\pi_y) \\ a^\dagger = \frac{1}{\sqrt{2\hbar e B}} (\pi_x + i\pi_y) \end{cases}, \quad (1.4)$$

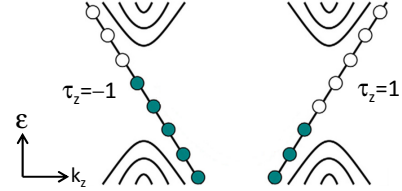


FIG. 1 For Weyl nodes with opposite helicities, the 0-th Landau levels slant toward opposite directions. The figure is from Hosur and Qi, 2013

then

$$[a, a^\dagger] = 1. \quad (1.5)$$

The Hamiltonian can be re-written as,

$$\mathbf{H} = \chi \hbar \omega (\sigma_+ a + \sigma_- a^\dagger) + \chi v \sigma_z \hbar k_z \quad (1.6)$$

$$= \chi \begin{pmatrix} v \hbar k_z & \hbar \omega a \\ \hbar \omega a^\dagger & -v \hbar k_z \end{pmatrix}, \quad (1.7)$$

where $\hbar \omega \equiv v \sqrt{2\hbar e B}$, and $\sigma_\pm = (\sigma_x \pm i\sigma_y)/2$.

We now solve

$$\mathbf{H} \Psi_n = \varepsilon_n \Psi_n, \quad (1.8)$$

$$\text{with } \Psi_n = u_n \begin{pmatrix} 1 \\ 0 \end{pmatrix} |n-1\rangle + v_n \begin{pmatrix} 0 \\ 1 \end{pmatrix} |n\rangle, \quad (1.9)$$

and $a|n\rangle = \sqrt{n}|n-1\rangle$, $a^\dagger|n\rangle = \sqrt{n+1}|n+1\rangle$. Then, for $n=0$, one has

$$\varepsilon_0^\chi = \chi v \hbar k_z. \quad (1.10)$$

For $n \geq 1$, one has

$$\begin{cases} v \hbar k_z u_n + \hbar \omega \sqrt{n} v_n = \chi \varepsilon_n u_n, \\ \hbar \omega \sqrt{n} u_n - v \hbar k_z v_n = \chi \varepsilon_n v_n. \end{cases} \quad (1.11)$$

To have non-trivial solutions, one needs

$$\det \begin{pmatrix} v \hbar k_z - \chi \varepsilon_n & \hbar \omega \sqrt{n} \\ \hbar \omega \sqrt{n} & -v \hbar k_z - \chi \varepsilon_n \end{pmatrix} = 0. \quad (1.12)$$

This gives

$$\varepsilon_{n\pm}^\chi = \pm \chi \hbar \omega \sqrt{n + (v k_z / \omega)^2}, \quad n \geq 1. \quad (1.13)$$

The energy dispersion of LLs along k_z (the direction of \mathbf{B}) are shown in Fig. 1. Notice that for Weyl nodes

with opposite helicities, the 0-th LLs slant toward opposite directions (along the direction of \mathbf{B}), parallel or anti-parallel to the magnetic field. *There is no energy dispersion within the plane perpendicular to the magnetic field.*

B. Weyl orbit

In previous Chapter, we studied the Fermi arc from the surface state. When coupled with the chiral LL in Eq. (1.10), they could form a continuous path of transport (Potter and Lee, 2011). Suppose there is a slab of Weyl semimetal with thickness L . The slab needs to be thin, so that the phase of an electron can remain coherent during the transport. However, it cannot be too thin, to avoid the coupling between the surface states from two sides. For simplicity, suppose the chemical potential equals the energy of the Weyl node.

Apply a perpendicular magnetic field $B\hat{y}$ to the slab, as shown in Fig. 2. An electron on the top Fermi arc has group velocity \mathbf{v} perpendicular to the arc. Because of the Lorentz force, the electron would move along the Fermi arc and reach a Weyl node. Beyond the adiabatic approximation, the surface state and the bulk state near the Weyl node could couple with each other. Thus the low-energy electron could hop to the chiral LL. Since the chiral LL has energy dispersion along the direction of \mathbf{B} , $\varepsilon_0^\pm = \pm\hbar vk_y$, the electron would move down to the bottom surface and hop on to the Fermi arc there. The Lorentz force drives the electron to the other Weyl node and the electron finally comes back up to complete a cycle. We will call such an orbit a **Weyl orbit**.

The energy quantum associated with an orbit with period T is h/T . Thus the Weyl orbit has the discrete energy spectrum,

$$\varepsilon_n = (n + \delta) \frac{h}{T}, \quad n = 0, 1, 2, \dots \quad (1.14)$$

where $0 \geq \delta < 1$, and the period $T = 2t_{arc} + 2t_{bulk}$. From the semiclassical equation of motion,

$$\hbar \dot{\mathbf{k}} = -e\mathbf{v} \times \mathbf{B}, \quad (1.15)$$

we have

$$\hbar k_A = evBt_{arc}, \quad (1.16)$$

where k_A is the length of the Fermi arc, and v is the speed in Eq. (1.1).

On the other hand, $t_{bulk} = \frac{L}{v}$, v is again the velocity in Eq. (1.1). Therefore,

$$\varepsilon_n = \frac{\hbar v}{2} \frac{n + \delta}{L + k_A \lambda_B^2}, \quad (1.17)$$

where $\lambda_B \equiv \sqrt{\hbar/eB}$ is the magnetic length. Note that the energy spectrum would depend on the thickness L .

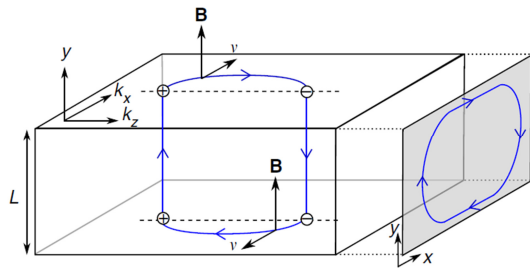


FIG. 2 Under a magnetic field, an electron slides along the Fermi arc on top, merge with the chiral LL of the bulk state at a Weyl point, then moves down, slides along the Fermi arc on bottom, and moves up to complete a cycle. Fig. from Potter *et al.*, 2014.

Similar to the analysis of the de Hass-van Alphen effect. The discrete energy levels would lead to a periodic variation of the density of states (DOS). When we fix μ but change B , the DOS would reach a local maximum whenever an energy level coincides with μ . As a result, in the plot of the DOS versus $1/B$, there is a period of oscillation,

$$\Delta \left(\frac{1}{B} \right) = \frac{\pi ev}{\mu k_A}. \quad (1.18)$$

Such an oscillation would reveal itself in various physical properties. For a review, see Zhang *et al.*, 2021.

C. Chiral anomaly

Consider a pair of Weyl nodes separated in momentum space (see Fig. 3(a)). We first apply a magnetic field, preferably along the line connecting the two nodes. Then, apply an additional electric field to push the electrons. If $\mathbf{E} \perp \mathbf{B}$, then the electrons won't move, since the LLs do not disperse along a direction perpendicular to \mathbf{B} . That is, only the component \mathbf{E}_{\parallel} parallel to \mathbf{B} could transport the electrons.

The electrons in the k_z -states of the 0-th LL slide along the z -direction with a rate (see Fig. 3(b)),

$$\frac{dQ_{\chi}^z}{dt} = (-e)\chi \frac{\frac{\Delta k_z}{2\pi/L_z}}{\Delta t} \quad (1.19)$$

$$= -e\chi \frac{\dot{k}_z}{2\pi/L_z}, \quad \hbar \dot{k}_z = -eE_z \quad (1.20)$$

$$= e^2 \chi \frac{E_{\parallel} L_z}{h}. \quad (1.21)$$

Furthermore, each LL has a huge degeneracy (see Chap 9 of Kittel, 2005),

$$D = \frac{\phi_{\text{tot}}}{\phi_0} = \frac{A_{\text{samp}} B}{h/e}, \quad (1.22)$$

which is the ratio between total magnetic flux (through the sample) and flux quantum $\phi_0 = h/e$. A_{samp} is the

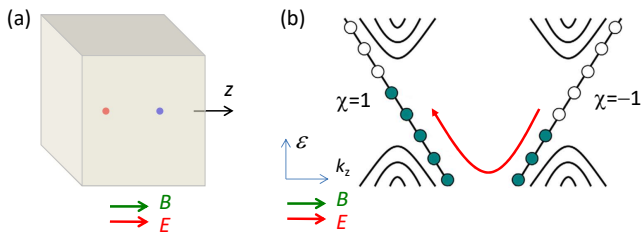


FIG. 3 (a) Applying a pair of electric and magnetic fields along the two Weyl nodes. (b) The magnetic field generates the chiral 0-th LLs in momentum space. The electric field pumps electrons from one node to another.

projected area of the sample perpendicular to \mathbf{B} . Therefore, the total charges transported via the 0-th LL are,

$$\frac{dQ_\chi^{3D}}{dt} = \frac{AB}{h/e} \frac{dQ_\chi^z}{dt} \quad (1.23)$$

$$= \chi \frac{e^3}{h^2} AL_z BE_{\parallel}. \quad (1.24)$$

For the chiral charge density, one has (Hosur and Qi, 2013; Nielsen and Ninomiya, 1983),

$$\frac{\partial \rho_\chi}{\partial t} = \chi \frac{e^3}{h^2} \mathbf{E} \cdot \mathbf{B}. \quad (1.25)$$

It is possible to get this result using a semiclassical analysis without discrete Landau levels (Stephanov and Yin, 2012). See Sec. I.F.4.

This is essentially the same as the equation for the **chiral anomaly** in particle physics (Adler, Bell, and Jackiw, 1969),

$$\partial_\mu J_5^\mu = -\frac{e^3}{h^2} \frac{1}{4} \varepsilon^{\mu\nu\rho\lambda} F_{\mu\nu} F_{\rho\lambda}, \quad (1.26)$$

where J_μ^5 is the chiral current density, and $J_5^0 = \rho_+ - \rho_-$. Note that in the context of particle physics, since there is no lattice in vacuum, there is no node doubling. Also, the Dirac sea of vacuum is not bounded from below, so the chiral charges are supplied from an infinite reservoir, not from the other node (which does not exist).

D. Chiral magnetic effect

Suppose that under a pair of \mathbf{E}, \mathbf{B} fields, the system is maintained in a steady state with different chemical potentials near the two nodes (see Fig. 4). Assume $\mu_+ > \mu_-$, and an electric field moves electron charges Q from right to left. The displacement of charges costs an energy,

$$dE = \frac{Q}{(-e)} (\mu_+ - \mu_-) > 0. \quad (1.27)$$

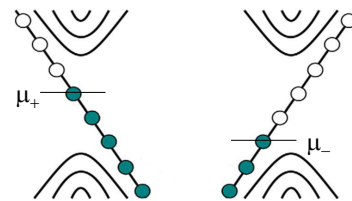


FIG. 4 In a non-equilibrium state, the chemical potentials near two nodes are different.

To balance the energy, the rate of work (per unit volume) done by the applied electric field should be

$$\mathbf{J} \cdot \mathbf{E} = \frac{dE/V}{dt} = \frac{1}{(-e)} \frac{\partial \rho}{\partial t} (\mu_+ - \mu_-) \quad (1.28)$$

$$= -\Delta\mu \frac{e^2}{h^2} \mathbf{E} \cdot \mathbf{B}, \quad (1.29)$$

where $\Delta\mu \equiv \mu_+ - \mu_-$.

Choose $\mathbf{E} \parallel \mathbf{B}$, and let $E \rightarrow 0$, then one seems to have,

$$\mathbf{J} = -\Delta\mu \frac{e^2}{h^2} \mathbf{B}. \quad (1.30)$$

This is called the **chiral magnetic effect** (CME). We will justify this using a semiclassical approach in Sec. I.F.3. The current vanishes when $\Delta\mu = 0$, so a non-equilibrium state is required. Suppose $B = 0.1$ T, and $\Delta\mu = 0.01$ meV, then the CME current J is about 0.01 (A/mm²). For a review of the CME, see Kharzeev and Liao, 2021.

Some remarks on the symmetries of the Hall effect and the chiral magnetic effect. From the symmetries of \mathbf{J} , \mathbf{E} , and \mathbf{B} , we can infer the symmetries of the transport coefficients:

$$\begin{array}{l} J_y = \sigma_H E_x \quad , \quad J_z = \alpha_B B_z \\ \text{SI} \quad - \quad + \quad - \quad - \quad - \quad + \\ \text{TR} \quad - \quad - \quad + \quad - \quad + \quad - \end{array}$$

The table above shows the change of signs of \mathbf{J} , \mathbf{E} , and \mathbf{B} under SI and TR. It follows that the Hall conductivity σ_H is even under SI, and odd under TR. The same symmetry holds also for longitudinal conductivity σ_L .

The Hall current is dissipationless, $\mathbf{J}_H \cdot \mathbf{E} = 0$. Therefore, in order for a system to have a non-zero σ_H , TRS needs be broken by applying a magnetic field or having magnetic materials. Note that for the longitudinal transport, the generation of the Joule heat, $\mathbf{J}_L \cdot \mathbf{E}$, would naturally break the TRS.

On the other hand, the CME coefficient α_B needs to be odd under SI, and even under TR. That is, the CME requires the breaking of SIS. This can be provided by the unbalanced chemical potentials near two Weyl nodes.

E. Negative magnetoresistance

Since a magnetic field tends to restrict the motion of electrons, the magnetoresistance (MR) is usually positive. That is, the resistance increases with the magnetic field. An exception is the disordered medium with **weak localization**. In this case, the localization is due to the phase coherence of electrons. A magnetic field breaks the phase coherence and delocalizes the electrons.

In Weyl semimetal, the charge pumping due to the chiral anomaly also would result in negative magnetoresistance. This is explained as follows. After allowing for the relaxation due to inter-node scatterings, the rate equation for chiral charges becomes,

$$\frac{\partial \rho_\chi}{\partial t} = \chi \frac{e^3}{\hbar^2} \mathbf{E} \cdot \mathbf{B} - \frac{\rho_\chi}{\tau_v}, \quad (1.31)$$

where τ_v is the inter-node scattering time. In steady state, $\partial \rho_\chi / \partial t = 0$, and one has

$$\rho_\pm = \pm \frac{e^3}{\hbar^2} \mathbf{E} \cdot \mathbf{B} \tau_v \quad (1.32)$$

$$\rightarrow \Delta \mu \propto \mathbf{E} \cdot \mathbf{B} \tau_v. \quad (1.33)$$

Because of the chiral magnetic effect, a non-zero chiral chemical potential leads to

$$\mathbf{J} = -\Delta \mu \frac{e^2}{\hbar^2} \mathbf{B} \quad (1.34)$$

$$\propto (\mathbf{E} \cdot \mathbf{B}) \mathbf{B} \tau_v. \quad (1.35)$$

When $\mathbf{E} \parallel \mathbf{B}$, the current, and thus the longitudinal conductivity, has a part proportional to B^2 . That is, we'll have a negative MR.

Furthermore, because of the $\mathbf{E} \cdot \mathbf{B}$ factor, when \mathbf{E} rotates away from \mathbf{B} , the current should reduce with the angle. Such a locking of the maximum current to the direction of the magnetic field is a signature of the chiral anomaly in Weyl semimetals (Xiong *et al.*, 2015).

F. Semiclassical analysis

We now study the transport in Weyl semimetals using a semiclassical approach. Not only the chiral magnetic effect, but also the chiral anomaly can be understood from such an approach.

1. Equation of motion

The semiclassical equations of motion for Bloch electron is valid under the one-band approximation – when interband transition can be ignored. For a non-degenerate Bloch band- n , we have (Xiao *et al.*, 2010),

$$\dot{\mathbf{r}} = \frac{\partial \tilde{\varepsilon}_{n\mathbf{k}}}{\hbar \partial \mathbf{k}} - \dot{\mathbf{k}} \times \boldsymbol{\Omega}_{n\mathbf{k}}, \quad (1.36)$$

$$\hbar \dot{\mathbf{k}} = -e\mathbf{E} - e\dot{\mathbf{r}} \times \mathbf{B}, \quad (1.37)$$

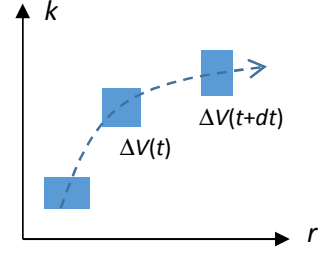


FIG. 5 Evolution of a volume element in phase space.

in which

$$\tilde{\varepsilon}_{n\mathbf{k}} \equiv \varepsilon_{n\mathbf{k}} - \mathbf{m}_{n\mathbf{k}} \cdot \mathbf{B} \quad (1.38)$$

is the energy of a Bloch wavepacket shifted by magnetic field. The electric and magnetic fields are allowed to vary slowly in space and time (compared to the lattice constant and the frequency ε_g/\hbar), but in the following discussion they are assumed to be static and uniform. The Berry curvature is,

$$\boldsymbol{\Omega}_{n\mathbf{k}} = i \left\langle \frac{\partial u_{n\mathbf{k}}}{\partial \mathbf{k}} \left| \times \right| \frac{\partial u_{n\mathbf{k}}}{\partial \mathbf{k}} \right\rangle, \quad (1.39)$$

and the magnetic moment of a Bloch electron is ($H_{\mathbf{k}} \equiv e^{-i\mathbf{k} \cdot \mathbf{r}} H e^{i\mathbf{k} \cdot \mathbf{r}}$),

$$\mathbf{m}_{n\mathbf{k}} = -\frac{e}{2\hbar} i \left\langle \frac{\partial u_{n\mathbf{k}}}{\partial \mathbf{k}} \left| \times \right| (H_{\mathbf{k}} - \varepsilon_{n\mathbf{k}}) \frac{\partial u_{n\mathbf{k}}}{\partial \mathbf{k}} \right\rangle. \quad (1.40)$$

Berry curvature $\boldsymbol{\Omega}_{n\mathbf{k}}$, magnetic moment $\mathbf{m}_{n\mathbf{k}}$, together with band energy $\varepsilon_{n\mathbf{k}}$, are three fundamental properties of Bloch states.

Combining Eqs. (1.36) and (1.37), one can get

$$D_n \dot{\mathbf{r}} = \mathbf{v}_n + \overbrace{\frac{e}{\hbar} \mathbf{E} \times \boldsymbol{\Omega}_n}^{\text{Hall effect}} + \overbrace{\frac{e}{\hbar} (\mathbf{v}_n \cdot \boldsymbol{\Omega}_n) \mathbf{B}}^{\text{CME}}, \quad (1.41)$$

$$D_n \hbar \dot{\mathbf{k}} = -e\mathbf{E} - e\mathbf{v}_n \times \mathbf{B} - e^2 (\mathbf{E} \cdot \mathbf{B}) \boldsymbol{\Omega}_n, \quad (1.42)$$

where $\mathbf{v}_n = \frac{\partial \varepsilon_{n\mathbf{k}}}{\hbar \partial \mathbf{k}}$, and

$$D_{n\mathbf{k}} \equiv 1 + \frac{e}{\hbar} \mathbf{B} \cdot \boldsymbol{\Omega}_{n\mathbf{k}}. \quad (1.43)$$

The second and the third terms in Eq. (1.41) are responsible for the Berry-curvature-related Hall effect and chiral magnetic effect respectively. In Eq. (1.42), in addition to the Lorentz force terms, the third term has something to do with the chiral anomaly. More details below.

2. Density of states in phase space

Consider a volume element in phase space moving along a trajectory,

$$\Delta V(t) = \Delta \mathbf{r}(t) \Delta \mathbf{k}(t), \quad (1.44)$$

where $\Delta\mathbf{r}$ is a shorthand notation for $\Delta x\Delta y\Delta z$, and similarly for $\Delta\mathbf{k}$. After a short time dt (Fig. 5),

$$\Delta\mathbf{r}(t+dt) = \Delta\mathbf{r}(t) + \Delta(\dot{x}dt)\Delta y\Delta z \quad (1.45)$$

$$\begin{aligned} &+ \Delta x\Delta(\dot{y}dt)\Delta z + \Delta x\Delta y\Delta(\dot{z}dt) \\ &\equiv \Delta\mathbf{r}(t) + \Delta\dot{\mathbf{r}}dt, \end{aligned} \quad (1.46)$$

and similarly for $\Delta\mathbf{k}(t+dt)$. Therefore,

$$\begin{aligned} \Delta V(t+dt) &= (\Delta\mathbf{r} + \Delta\dot{\mathbf{r}}dt)(\Delta\mathbf{k} + \Delta\dot{\mathbf{k}}dt) \\ &= \Delta\mathbf{r}\Delta\mathbf{k} + \Delta\mathbf{r}\Delta\dot{\mathbf{k}}dt + \Delta\dot{\mathbf{r}}dt\Delta\mathbf{k} + O(\Delta^2). \end{aligned} \quad (1.47)$$

It follows that,

$$\frac{d\Delta V}{dt} = \left(\frac{\Delta\dot{\mathbf{r}}}{\Delta\mathbf{r}} + \frac{\Delta\dot{\mathbf{k}}}{\Delta\mathbf{k}} \right) \Delta V \quad (1.48)$$

$$= (\nabla_{\mathbf{r}} \cdot \dot{\mathbf{r}} + \nabla_{\mathbf{k}} \cdot \dot{\mathbf{k}}) \Delta V. \quad (1.49)$$

Replace $\dot{\mathbf{r}}, \dot{\mathbf{k}}$ with the right-hand sides of Eqs. (1.36) and (1.37), and neglect higher-order gradient terms such as $\frac{\partial m}{\partial \mathbf{k}} \frac{\partial \mathbf{B}}{\partial \mathbf{r}}$, you should be able to get

$$\nabla_{\mathbf{r}} \cdot \dot{\mathbf{r}} + \nabla_{\mathbf{k}} \cdot \dot{\mathbf{k}} = -\frac{1}{D} \frac{dD}{dt} - \frac{e^2}{\hbar^2} \frac{\mathbf{E} \cdot \mathbf{B}}{D} \nabla_{\mathbf{k}} \cdot \boldsymbol{\Omega}. \quad (1.50)$$

The divergence of the Berry curvature is zero as long as a trajectory stays away from regions with level-degeneracy. It follows from Eq. (1.49) that if $\nabla_{\mathbf{k}} \cdot \boldsymbol{\Omega} = 0$, then $D\Delta V$ is a constant of motion,

$$\left(1 + \frac{e}{\hbar} \mathbf{B} \cdot \boldsymbol{\Omega}\right) \Delta V = \Delta V_0, \quad (1.51)$$

where ΔV_0 is the volume element in the absence of the correction. That is, D (which depends on $\boldsymbol{\Omega}$ and \mathbf{B}) modifies the density of states in phase space.

After the modification, the number of particles in ΔV is $f(\mathbf{r}, \mathbf{k}, t)D(\mathbf{r}, \mathbf{k})\Delta V/(2\pi)^3$, where f is the Fermi-Dirac distribution function. Thus, the particle density in *phase space* is

$$\tilde{n}(\mathbf{r}, \mathbf{k}, t) = D(\mathbf{r}, \mathbf{k})f(\mathbf{r}, \mathbf{k}, t)/(2\pi)^3. \quad (1.52)$$

The particle density in *real space* is

$$n(\mathbf{r}, t) = \int \frac{d^3k}{(2\pi)^3} D(\mathbf{r}, \mathbf{k})f(\mathbf{r}, \mathbf{k}, t). \quad (1.53)$$

3. Chiral magnetic effect

According to Eq. (1.41), in the presence of a magnetic field, the current density,

$$\mathbf{J}(\mathbf{r}) = -e \int \frac{d^3k}{(2\pi)^3} f D_n \dot{\mathbf{r}} \quad (1.54)$$

$$= -\frac{e^2}{\hbar} \underbrace{\int \frac{d^3k}{(2\pi)^3} f \mathbf{v}_n \cdot \boldsymbol{\Omega}_n}_{=\alpha_B} \mathbf{B}. \quad (1.55)$$

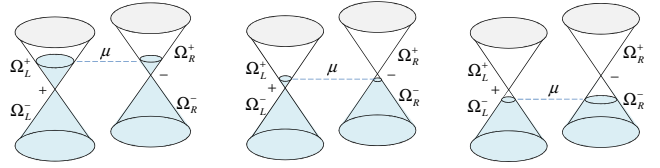


FIG. 6 The Berry flux through the Fermi surfaces of a pair of Weyl nodes is zero no matter whether the chemical potential is above, between, or below a pair of nodes.

The same result can be obtained with the theory of linear response under the static limit (Chang and Yang, 2015a).

From this result, it appears that a current would be flowing along \mathbf{B} with a coefficient α_B . However, there is a simple argument against *static* CME for a system in equilibrium (Başar et al., 2014). It is known that the rate of mechanical work done by an EM field on charges (per unit column) is $\mathbf{J} \cdot \mathbf{E}$. This is what causes the Joule heat. Now, if $\mathbf{J} = \alpha_B \mathbf{B}$, then

$$\frac{dW}{dt} = \mathbf{J} \cdot \mathbf{E} = \alpha_B \mathbf{E} \cdot \mathbf{B}, \quad (1.56)$$

which can be positive or negative, depending on the sign of $\mathbf{E} \cdot \mathbf{B}$. That is, it is possible to extract energy from an equilibrium system, which is unreasonable. Therefore, there should be no *static* CME for systems in equilibrium.

In fact, one can show that the integral of α_B is zero for systems in equilibrium (Zhou et al., 2013). First, recall that

$$\int \frac{d^3k}{(2\pi)^3} f = \frac{1}{(2\pi)^3} \int d\varepsilon \int \frac{d^2S}{|\partial\varepsilon/\partial\mathbf{k}|} f, \quad (1.57)$$

in which d^2S integrates over a constant-energy surface. Therefore, one can rewrite the integral in α_B as,

$$\begin{aligned} \int_{\text{filled}} d^3k f \mathbf{v}_n \cdot \boldsymbol{\Omega}_n &= \frac{1}{(2\pi)^3} \frac{1}{\hbar} \int^\mu d\varepsilon f \int d^2S \frac{\mathbf{v}_n \cdot \boldsymbol{\Omega}}{v_n} \\ &= \frac{1}{(2\pi)^3} \frac{1}{\hbar} \int^\mu d\varepsilon f \underbrace{\int d^2\mathbf{S} \cdot \boldsymbol{\Omega}}_{=\Phi_\Omega(\varepsilon)}. \end{aligned} \quad (1.58)$$

The surface integral gives the Berry flux $\Phi_\Omega(\varepsilon)$ through a isoenergy surface. If the surface surrounds a Weyl node with chirality χ , then $\Phi_\Omega = 2\pi\chi$.

If the energy ε is above a Weyl point, then there is an electron pocket surrounding the Weyl point, and \mathbf{v} points out. If the energy ε is below a Weyl point, then there is a hole pocket surrounding the Weyl point, and \mathbf{v} points in. On the other hand the Weyl cones above and below the Weyl point have $\boldsymbol{\Omega}$'s with opposite signs. Therefore, no matter whether ε is above or below the Weyl point, the Berry fluxes are the same for a given node, $\Phi_\Omega(\varepsilon) = 2\pi\chi$.

Since the Weyl points always appear in pairs with opposite chiralities, it follows that no matter what ε is, the total Berry fluxes passing through an energy shell (with

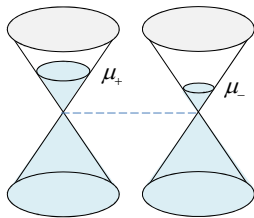


FIG. 7 The chemical potentials near two Weyl nodes in non-equilibrium state.

several pieces of isoenergy surfaces) with energy ε is always zero (Fig. 6). The CME coefficient α_B is an integral of $\Phi_\Omega(\varepsilon)$ over energy, but the result remains to be zero since $\Phi_\Omega(\varepsilon) = 0$ for each energy shells.

However, if the chemical potentials of two Weyl cones, μ_+ and μ_- , are not the same, then the cancellation is not complete (Fig. 7). Suppose $\mu_+ > \mu_-$, then

$$\begin{aligned} & \int^{\mu_+} d\varepsilon \int d^2\mathbf{S} \cdot \boldsymbol{\Omega} + \int^{\mu_-} d\varepsilon \int d^2\mathbf{S} \cdot \boldsymbol{\Omega} \\ &= \int_{\mu_-}^{\mu_+} d\varepsilon \int d^2\mathbf{S} \cdot \boldsymbol{\Omega} = 2\pi(\mu_+ - \mu_-). \end{aligned} \quad (1.59)$$

It follows that,

$$\mathbf{J} = -\Delta\mu \frac{e^2}{\hbar^2} \mathbf{B}. \quad (1.60)$$

Note: If the magnetic field is time-dependent, then there can be CME even if the system is originally in equilibrium. This is the *dynamic* chiral magnetic effect. The expression for dynamic α_B is different from the one above. This dynamic CME is closely related to natural optical gyrotropic effect (Zhong *et al.*, 2016), and does not even require the existence of Weyl nodes (Chang and Yang, 2015b).

4. Chiral anomaly

From $\tilde{n} = Df/(2\pi)^3$ and Eq. (1.50), we can also have

$$\frac{\partial \tilde{n}}{\partial t} + \nabla_r \cdot (\tilde{n} \dot{\mathbf{r}}) + \nabla_k \cdot (\tilde{n} \dot{\mathbf{k}}) = -\frac{e^2}{\hbar^2} \mathbf{E} \cdot \mathbf{B} f \nabla_k \cdot \boldsymbol{\Omega} + D \frac{df}{dt}. \quad (1.61)$$

The last term is zero in the absence of collision,

$$\frac{df}{dt} = \frac{\partial f}{\partial t} + \dot{\mathbf{r}} \cdot \nabla_r f + \dot{\mathbf{k}} \cdot \nabla_k f = 0, \quad (1.62)$$

which is the collisionless Boltzmann equation. Thus, the equation of continuity is,

$$\frac{\partial \tilde{n}}{\partial t} + \nabla_r \cdot (\tilde{n} \dot{\mathbf{r}}) + \nabla_k \cdot (\tilde{n} \dot{\mathbf{k}}) = -\frac{e^2}{\hbar^2} \mathbf{E} \cdot \mathbf{B} f \nabla_k \cdot \boldsymbol{\Omega}. \quad (1.63)$$

The source/sink term on the right-hand side of the equation is related to the divergence of the Berry curvature. Since the Berry curvature $\boldsymbol{\Omega}(\mathbf{k})$ is like the "magnetic" field in momentum space, its divergence can be

nonzero only if there is a "monopole" from a Weyl point inside the Brillouin zone. Integrate Eq. (1.63) over momentum (at $T = 0$), one then has

$$\frac{\partial n}{\partial t} + \nabla_r \cdot \mathbf{J}_n = -\frac{e^2}{\hbar^2} \mathbf{E} \cdot \mathbf{B} \underbrace{\frac{1}{2\pi} \int d\mathbf{S}_k \cdot \boldsymbol{\Omega}}_{=\chi}, \quad (1.64)$$

where χ is the chirality of the Weyl point. The equation for charge density, $\rho = -en$, is,

$$\frac{\partial \rho}{\partial t} + \nabla_r \cdot \mathbf{J} = \chi \frac{e^3}{\hbar^2} \mathbf{E} \cdot \mathbf{B}, \quad (1.65)$$

This is the equation for chiral anomaly in Eq. (1.25).

Exercise

1. (a) From the semiclassical equations of motion, derive Eq. (1.50).
- (b) With the help of the equation above, derive Eq. (1.61).

REFERENCES

- Chang, Ming-Che, and Min-Fong Yang (2015a), "Chiral magnetic effect in a two-band lattice model of weyl semimetal," Phys. Rev. B **91**, 115203.
- Chang, Ming-Che, and Min-Fong Yang (2015b), "Chiral magnetic effect in the absence of weyl node," Phys. Rev. B **92**, 205201.
- Başar, Gök çe, Dmitri E. Kharzeev, and Ho-Ung Yee (2014), "Triangle anomaly in weyl semimetals," Phys. Rev. B **89**, 035142.
- Hosur, Pavan, and Xiaoliang Qi (2013), "Recent developments in transport phenomena in weyl semimetals," Comptes Rendus Physique **14** (9–10), 857 – 870.
- Kharzeev, Dmitri E, and Jinfeng Liao (2021), "Chiral magnetic effect reveals the topology of gauge fields in heavy-ion collisions," Nature Reviews Physics **3** (1), 55–63.
- Kittel, Charles (2005), *Introduction to Solid State Physics*, 8th ed. (John Wiley & Sons, Inc.).
- Nielsen, H B, and Masao Ninomiya (1983), "The adler-bell-jackiw anomaly and weyl fermions in a crystal," Phys. Lett. B **130** (6), 389.
- Potter, Andrew C, Itamar Kimchi, and Ashvin Vishwanath (2014), "Quantum oscillations from surface fermi arcs in weyl and dirac semimetals," Nature Communications **5**, 5161.
- Potter, Andrew C, and Patrick A. Lee (2011), "Engineering a $p+ip$ superconductor: Comparison of topological insulator and rashba spin-orbit-coupled materials," Phys. Rev. B **83**, 184520.
- Stephanov, M A, and Y. Yin (2012), "Chiral kinetic theory," Phys. Rev. Lett. **109**, 162001.
- Xiao, Di, Ming-Che Chang, and Qian Niu (2010), "Berry phase effects on electronic properties," Rev. Mod. Phys. **82**, 1959–2007.
- Xiong, Jun, Satya K. Kushwaha, Tian Liang, Jason W. Krizan, Max Hirschberger, Wudi Wang, R. J. Cava, and N. P. Ong (2015), "Evidence for the chiral anomaly in the dirac semimetal na3bi," Science **350** (6259), 413–416.

- Zhang, Cheng, Yi Zhang, Hai-Zhou Lu, X. C. Xie, and Faxian Xiu (2021), “Cycling fermi arc electrons with weyl orbits,” *Nature Reviews Physics* **3** (9), 660–670.
- Zhong, Shudan, Joel E. Moore, and Ivo Souza (2016), “Gyrotropic magnetic effect and the magnetic moment on the fermi surface,” *Phys. Rev. Lett.* **116**, 077201.
- Zhou, Jian-Hui, Hua Jiang, Qian Niu, and Jun-Ren Shi (2013), “Topological invariants of metals and the related physical effects,” *Chinese Physics Letters* **30** (2), 027101.
- Zyuzin, A A, and A. A. Burkov (2012), “Topological response in weyl semimetals and the chiral anomaly,” *Phys. Rev. B* **86**, 115133.